COBEM 2023 27TH INTERNATIONAL CONGRESS OF MECHANICAL ENGENEERING

ABCM Brazilian Society of Mechanical Sciences and Engineering
27th ABCM International Congress of Mechanical Engineering
December 04-08, 2023, Florianópolis-SC, Brazil

COB-2023-1202

Optimization of the LQR and SDRE control scheme for a non-linear semi-active MR damper on a quarter vehicle model

Leonardo da Costa Rodrigues Ferreira
Depto. Automotive Engineering, University of Brasília, Campus Gama, Brasília/DF
rodrigues.ferreira@aluno.unb.br

Marcus V. G. de Morais
Depto. Mechanical Engineering, University of Brasilia, Campus Darcy, Brasília/DF
mvmorais@unb.br

Abstract. *This work aims to compare the behavior of a semi-active suspension on a quarter vehicle model using the Linear-Quadratic Regulator (LQR) control scheme and one of its non-linear variations (State Dependent Riccati Equation - SDRE) per report to a passive suspension system. The semi-active suspension mathematical model is based upon equations of physically motivated models present in the literature, incorporating nonlinear behaviors such as force hysteresis and asymmetry. Due to this complex relationship between force and speed, the LQR technique is considered sub-optimal regarding control, leading to the deployment of better suited alternatives such as the SDRE technique to gauge the degree of inadequacy. To measure performance to form the basis for the comparisons, the movement of the vehicle is characterized using the H_2 metric of the upper body and the H_∞ metric of the lower body, also known as the RMS gain and roadhold of the vehicle. A Gaussian white noise function is used for the road profile. The systems are evaluated using numerical integration methods. An optimization on the free parameters of the suspension control is performed by means of the NSGA-II Genetic Algorithm. The Pareto optimums of the metrics for the evaluated systems for each control scheme is found, with the system showing robustness with regards to the controller parameters. The SDRE control scheme showed better performance in both evaluated metrics, having significantly better H_2 results.*
Keywords: *Semi-active vehicle suspension, non linear control, LQR controller, SDRE control, Multi-objective Optimization, Genetic Algorithm, MR damper*

1. Introduction

The suspension is an important vehicle system to isolate the chassis from the road oscillations. Many works in the literature seek to characterize the dynamics of a vehicle through the use of performance metrics, be it using a quarter vehicle model (Melo, 2017; Ferreira *et al.*, 2022; Li *et al.*, 2021), half vehicle (Wei and Taghavifar, 2017; de Lima *et al.*, 2012), or full vehicle (Shirahatti *et al.*, 2009).

The optimal passive suspension is known in the literature for most cases, as for example the optimal quarter vehicle suspension in Gillespie (1992). Given the desire to improve suspension properties, those articles usually study the use of a active or semi-active suspension, with control schemes such as the Skyhook (Melo, 2017), PID (Li *et al.*, 2021) and LQR (Chen *et al.*, 2014) being employed on quarter vehicles.

For the LQR, the main challenge lies in the tuning of weights matrices L and Q (Gawronski, 2004). While the former deals with the issue through a manual iterative approach, that's unsuitable for large systems or large quantities of systems. The most common approach in modern works is to use an optimization algorithm to obtain the desired weights. Saleem (2022) used a gradient descent algorithm. Morar and Dobra (2021) used an Artificial Bee Colony optimization algorithm to tune it's LQR weights. Prabakar *et al.* (2016), Koch (2011), Nagarkar and Vikhe (2016) all used genetic algorithms. They're of special interest as they also performed their optimization weights for the control of vehicle suspensions.

The SDRE is an algorithm based on the LQR control that is modified to better handle non-linear systems. It shares the general structure of the LQR technique including the challenges of tuning the weights, but has additional dynamics in the form of non-linear parametrizations. For decades, many articles show it's potential to regulate the vibration levels of non-linear systems, both in the theoretical (Cloutier, 1997; Cloutier *et al.*, 1996; Çimen, 2010) and applied (Stansbery and Cloutier, 2001; Itik *et al.*, 2010; Aguilar-Ibanez *et al.*, 2022; Do *et al.*, 2012) fields. In the field of vehicle dynamics, Kilicaslan (2022) used the technique to tune an active suspension system for a quarter vehicle model with non-linearities, while Acarman (2009) used the technique to control the lateral dynamics of a quarter vehicle for braking. Neither, however, optimized the weight matrices, opting for values based on their system's equations of motion instead.

Owing to the prevalence of this technique in the literature, the optimization of multi-objective problems was performed via the Non sorting Genetic Algorithm II (NSGA-II) (Deb *et al.*, 2000).

This work aims to compare the behavior of a semi-active suspension on a quarter vehicle model using the LQR control scheme and one of its non-linear variations, SDRE, to a passive suspension system. The semi-active suspension mathematical model is based upon equations of physically motivated models present in the literature, incorporating nonlinear behaviors such as force hysteresis and asymmetry. Due to this complex relationship between force and speed, the LQR technique is considered sub-optimal regarding control, leading to the deployment of better suited alternatives such as the SDRE technique to gauge the degree of inadequacy.

To measure performance to form the basis for the comparisons, the movement of the vehicle is characterized using the H_2 metric of the upper body and the H_∞ metric of the lower body, also known as the RMS gain and roadhold of the vehicle, respectively. A Gaussian white noise function is used as the road profile. The systems are evaluated using numerical integration methods. An optimization on the free parameters of the suspension control is performed by means of the NSGA-II Genetic Algorithm. The Pareto optimums of the metrics for the evaluated systems for each control scheme as well as the sensibility of the metrics value to changes in its parameters when near the optimum are found.

2. Quarter of vehicle Semi-Active with MR-Damper

The quarter vehicle model is commonly used in the literature to examine the effects of certain parameters on vehicle handling. From it the equations of motion for the upper and lower bodies Eq. (1) are derived. Using the subscript "s" to denote the upper, sprung body and "u" to denote the lower, unsprung body, Eq. (1) becomes:

$$\begin{bmatrix} M_s & 0 \\ 0 & M_u \end{bmatrix} \begin{bmatrix} \ddot{x}_s \\ \ddot{x}_u \end{bmatrix} + \begin{bmatrix} c_s & -c_s \\ -c_s & c_s \end{bmatrix} \begin{bmatrix} \dot{x}_s \\ \dot{x}_u \end{bmatrix} + \begin{bmatrix} k_s & -k_s \\ -k_s & k_s + k_u \end{bmatrix} \begin{bmatrix} x_s \\ x_u \end{bmatrix} = \begin{bmatrix} 0 \\ zk_u \end{bmatrix} + \begin{bmatrix} F \\ -F \end{bmatrix} \tag{1}$$

where k_s and k_u denotes the spring stiffness of suspension and tires, respectively; c_s is the damper coefficient of suspension system; M_s and M_u are the sprung and unsprung (tire) masses, respectively, F is the imposed force on the sprung and unsprung masses; z the road profile; and x the vehicle position. The variables "z" and "x" are time dependent. The variable "c_s" is also time dependent for semi-active suspension systems. Lastly, the variable F is time dependent for an active suspension, being null otherwise. The MR suspension forces can also be represented there instead of in the c_s term, making it not zero in the case of a semi-active suspension. Equation (1) is an ordinary differential equation for the system. This equation can also be represented in the state space form, as described below:

$$\dot{\mathbf{x}} = \mathbf{Ax} + \mathbf{Bu} + \mathbf{Cz} \tag{2}$$

where the state matrix **A** multiply with state variables $\mathbf{x} = [x_s \; x_u]^T$ (the quarter vehicle coordinate variables), **Bu** contains the terms relating to controllable forces, and **Cz** contains the excitation (random input) forces (Ogata, 2011).

2.1 Wang's Sigmoid MR-Damper Model

A MR-damper consists in a damper whose properties are partially controllable. The semi-active system is controlled by solving the system with no force constraints and reproducing it to the extent which it is possible by the varying damper force. The specific MR damper's formulation belongs to the double Sigmoid modeling family (Wang *et al.*, 2004). The choice of this specific model was motivated by the perceived better agreement with the experimental data compared to other models (Santade, 2017; Silva *et al.*, 2022).

The Wang's sigmoid formulation (Wang *et al.*, 2004) for the MR damper is described by

$$F(\dot{v}) = f_t \frac{1 - e^{F_1(\dot{v})}}{1 + e^{F_1(\dot{v})}} (1 - k_5)(1 + F_2(\dot{v})) \tag{3}$$

where $\dot{v}$ is the relative speed $x_s - x_u$, k_5 is a constant, f_t is the expression in 4, $F_1(\dot{x})$ is the expression in 5 and $F_2(\dot{x})$ is the expression in 6.

$$f_t = f_0(1 + e^{a_1 v_m}) \left(1 + \frac{k_2}{1 + e^{-a_2(i+I_0)}} - \frac{k_2}{1 + e^{-a_2(I_0)}} \right) \tag{4}$$

where a_1, k_2, I_0 and f_0 are constants, i is the controlled current passing through the damper coils, and v_m is the peak velocity of the damper. Due to numerical issues that arise from the expression provided in the paper for v_m under random excitation, an alternative expression for v_m was used that is consistent with the results in the original paper but better reflects the dynamics of the damper under white noise, as proposed in Ferreira *et al.* (2023).

$$F_1(\dot{v}) = -\frac{a_0}{1 + k_0 v_m} \left((\dot{v}) + sgn(\ddot{v}) k_4 v_m (1 + \frac{k_3}{1 + e^{-a_3(i+I_1)}} - \frac{k_3}{1 + e^{-a_3(I_1)}}) + k_6 v_m \right) \tag{5}$$

where a_0, a_3, k_0, k_3, k_4, k_6 and I_1 are constants and $sgn(\ddot{x})$ is the sign function of the relative acceleration $\ddot{v}$ defined by the expression $\ddot{x}_s - \ddot{x}_u$,.

$$F_2(\dot{v}) = |(\dot{v})|e^{-a_4 v_m}\left(\frac{1+sgn(\dot{v})}{2}k_{1c} + \frac{1-sgn(\dot{v})}{2}k_{1e}\right) \tag{6}$$

where a_4, k_{1c} and k_{1e} are constants.

The semi-active damping model employed used the data from Wang *et al.* (2004) with the K_1 coefficients modified as per Ferreira (2022), as displayed in Table 1. The baseline force f_0 was scaled for the mass differences as suggested in the original article.

Table 1. Data for the magneto-rheological damper contained in Wang *et al.* (2004), with the K_{1c} and K_{1e} values modified as per Ferreira (2022).

Constant	Value	Constant	Value	Constant	Value	Constant	Value
a_0 (adm)	1300	$a_4\ (m/s)^{-1}$	4.60	k_0 (adm)	112.5	k_3 (adm)	2.90
$a_1\ (m/s)^{-1}$	1.75	I_0 (amp)	0.05	k_{1c} (adm)	3.2	k_4 (adm)	0.095
$a_2\ (amp)^{-1}$	2.85	I_1 (amp)	0.08	k_{1e} (adm)	3.2	k_5 (adm)	0.65
$a_3\ (amp)^{-1}$	1.55	f_0 (N)	214.8	k_2 (adm)	19.4	k_6 (adm)	0.12

A interesting property of the MR damper is that, under certain conditions, it can actually exert a positive or negative force depending on the current. In those specific regions, it is able to reproduce the forces of active controllers better than idealized semi-active dampers that lack this property.

2.2 Optimization Metrics for Comfort and Handling

The solution of this problem using this system of equations can be found in Gillespie (1992). This analytical solution has been used to validate the numerical model for a passive damper system in a previous work (Ferreira *et al.*, 2022). In said work, a numerical study on the sensibility of the control metric on the variation of the spring parameters was done for a semi-active suspension using the Skyhook and Groundhook control techniques.

The two metrics analyzed are: (a) the H_2 metric for the sprung mass movement and (b) the H_∞ for the unsprung mass movement (Gawronski, 2004). The H_2 metric, also referred to as the RMS value of the gain, is expressed as:

$$RMS(G_i) = H_2(x_i) = S\int_0^\infty |G_i(\omega)|^2 d\omega \tag{7}$$

where S is the spectral density of the white noise that serves as input, and G_i the transfer (gain) function of quarter vehicle model for x_i as function of frequency ω. The chosen variable x in the quarter vehicle is usually x_s, thus measuring how comfortable the ride is for the vehicle passengers. Many of the previously mentioned works seek to minimize this value (Shirahatti *et al.*, 2009; Zhang *et al.*, 2012; Ferreira *et al.*, 2022).

The roadhold property is defined as the H_∞ metric on the unsprung mass. This is because the gain on the unsprung mass determines how close it is to losing contact with the ground (Gomes and de Morais, 2021; Gillespie, 1992). If this value surpasses 1 it means that the tire has lost it's ability to control the vehicle trajectory, representing a safety risk.

$$rh(G_u) = H_\infty(x_u) - 1 = max(\frac{x_u - z}{z}) = max(H_2(\omega, x_u) - 1)) \tag{8}$$

where rh is the value of the roadhold.

The optimizations can be performed by searching the space of admissible properties for a desired quality Gomes and de Morais (2021); Ferreira *et al.* (2022). When optimizing the H_2 metric, the purpose is posed as minimizing the value f_1 such as in equation (9).

$$f_1 = RMS\left[H_2(K, C)\right] \tag{9}$$

For optimizing the H_∞ metric, it's desirable to find the lowest value for the Roadhold peak, which leads to minimizing the expression in equation (10).

$$f_2 = rh\left[G_2(K, C))\right] \tag{10}$$

3. Control Strategies

3.1 LQR control

The LQR control is the basis of the techniques to be employed. It's a technique which obtains the optimal control of linear plants subject to disturbances. Gawronski (2004) demonstrates how the algorithm for the method can be derived while Md Sam *et al.* (2000) demonstrates it's application on a vehicle with an active suspension. A LQR controller seeks a gain L (11) so that Eq. (12) is satisfied and minimized. This is guaranteed by constructing L in the form expressed by Eq. (13). It's assumed that the system is analyzed on an timescale which approaches infinity, and as such the constant term outside the integral which would otherwise be present is discarded. Furthermore, the system is taken as continuous.

$$u = -Lx \tag{11}$$

$$J = \int_0^\infty x^T Q x + u^t R u \, dt \tag{12}$$

$$L = R^{-1} B^T P \tag{13}$$

where, x is the state vector; u is the force F applied on the structure; **B** is the input matrix (2); **L** is the gain matrix; **R** and **Q** are the weighting matrices that minimize the value **J**, and the matrix **P** is the matrix which satisfies the reduced-matrix Riccati equation:

$$\mathbf{A}^T\mathbf{P} + \mathbf{PA} - \mathbf{PBR}^T\mathbf{B}^T\mathbf{P} + \mathbf{Q} = 0 \tag{14}$$

where **A** and **B** are the same state and input matrices as described in equation (2).

The matrices **Q** and **R** are assumed to be know prior to performing the calculations, and finding the optimal values for said matrices is one of the central challenges when employing the LQR method. As put by Gawronski (2004), "this task does not have an analytical solution in general, and is frequently solved using a trial-and-error approach".

A modification done in order to better handle the system non-linearities was a velocity corrective term for the variable $\dot{x}_s$. Because of the asymmetric behavior of the damper relative to it's speed due to the term $k_6 v_m$, the damper equilibrium position occurs at non-zero displacements and speeds relative to it's initial conditions. To account for this asymmetry, the control unit was fed a modified upper body velocity $x_s - k_6 v_m$, which when fed to the controller provided significantly better results as the equilibrium point was correctly identified as not being in the origin.

3.2 SDRE variant

In the SDRE method, the matrices A and B from equation (14) are parameterized as functions of x, as demonstrated in Çimen (2010). This makes Eq. (14) take the form of Eq. (15). Due to this parametrization, this method is far more suited to control non-linear systems.

$$\mathbf{A(x)}^T\mathbf{P} + \mathbf{PB(x)} - \mathbf{PA(x)R}^T\mathbf{B(x)}^T\mathbf{P} + \mathbf{Q} = 0 \tag{15}$$

Unlike in the LQR case, this equation needs to be solved in every time step the controller acts, as the matrices A(x) and B(x) are liable to change as x changes. This makes the SDRE method more computationally intensive. The algorithm for calculating the SDRE is demonstrated in Fig. (1).

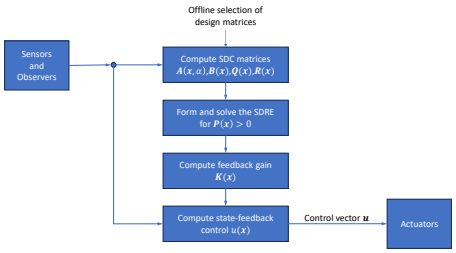

Figure 1. Algorithm procedures for calculation of the SDRE control. Reproduced from Çimen (2010).

The SDRE parametrization chosen was the derivative of the damping function in Eq. (3) with respect to the relative velocity $\dot{v}$. It was calculated using a computer-based derivative calculator, and due to it's cumbersome size it's not feasible to show it, thus it is omitted. Denoting such derivative as $f(\dot{v})$, the expression for A(x) in the space state form is given as equation 16. Given the lack of non-linear dynamics in the B matrix, there was no SDRE parametrization done to it. This parametrization is similar to the SDC parametrization.

$$A(x)x = \left(\begin{bmatrix} 0 & 0 & 1 & 0 \\ 0 & 0 & 0 & 1 \\ -\frac{K_s}{m_s} & \frac{K_s}{m_s} & 0 & 0 \\ \frac{K_s}{m_u} & -\frac{K_s+K_u}{m_u} & 0 & 0 \end{bmatrix} + \begin{bmatrix} 0 & 0 & 0 & 0 \\ 0 & 0 & 0 & 0 \\ 0 & 0 & -\frac{f(\dot{v})}{m_s} & \frac{f(\dot{v})}{m_s} \\ 0 & 0 & \frac{f(\dot{v})}{m_u} & -\frac{f(\dot{v})}{m_u} \end{bmatrix} \right) \begin{bmatrix} x_s \\ x_u \\ \dot{x}_s \\ \dot{x}_u \end{bmatrix} \tag{16}$$

4. Optimization strategies for the SDRE and LQR control schemes

4.1 Optimization and model parameters

In the literature, the optimization is almost universally performed using genetic algorithms, with a high preference towards the NSGA-II, specially in multi-objective optimizations. For this reason the NSGA-II was chosen. As for the optimization targets, the choice of minimizing the H_2 and H_∞ metrics was made due to their importance on vehicle performance and presence in the literature. To prevent excessive displacements, a limit of 10 cm for the suspension displacement was also enforced as a constraint.

The system was modeled using Simulink and Matlab. The numerical integrator of choice was the ODE45 owing to it's good precision and performance. The non-uniform fast Fourier transform was performed on the time domain results, with the frequency domain results up to 100 Hz being analyzed.

An individual run consists of the vehicle being simulated from null initial conditions under a band limited random noise input in the lower body, with 10^{-8} W of power and a cut-off frequency of 2 000 Hz. The system was granted 6 seconds to reach steady state and then had it's results logged for 8 more, providing a resolution of 0,25 Hz in the frequency domain when taking a Fourier transform (Proakis and Manolakis, 1996). The 2 000 Hz was also the simulation speed for the MR damper, as further decreases yielded no changes in the behavior. This also set the minimum simulation rate to 2 000 Hz, avoiding issues with frequency aliasing in the Fourier transform as well.

To account for the random nature of the road input, each individual was ran 22 times, and the resulting H_2 and H_∞ metrics were taken as the average values of the individual metrics for each run.

The controller ran on 50 ms update intervals. As put by Çimen (2010), "SDRE control laws can be implemented at speeds greater than 600 Hz and up to 2 kHz sample rates, [...] using commercial, off-the-shelf processors.". As such, a 200 Hz implementation is within reasonable bounds.

The number of individuals in each generation was 200, and 50 generations were ran. These parameters were tested for the objectives of minimizing the RMS and roadhold of the upper mass and were found to be adequate, obtaining convergence. Due to issues perceived early on with the system's performance if values in the weight matrices were too big, the maximum value for the weight variables was 5000. The cross-over chance was 90% and the mutation chance was 10%.

Table 2. Properties of the optimization

Property	Value	Property	Value
Integrator	ODE45	Steady state interval	6 seconds
Minimum simulation frequency	2000 Hz	Simulation time	8 seconds
White noise band cut-off	2000 Hz	Frequency analysis range	100 Hz
Damper simulation frequency	2000 Hz	Number of frequency averages	22
Controller update frequency	200 Hz	Population size	200
White noise power	10^{-8} W	Number of generations	50
Minimum value for Q/R	>0	Maximum value for Q/R	<5000

4.2 Optimization of LQR parameters

In the simple LQR case, the cost matrix is optimized as in Eq. (17),

$$\mathbf{R} = \mathbf{R}_0 \tag{17}$$

in which R_0 is just a matrix with constant terms. This is the most traditional implementation of the system, with the solution to the Ricatti equation only needing to be performed once.

In order for a positive, semi-definite solution for P in Eq. (14) to always exists, both Q and R also need to be positive definite (Çimen, 2010). This wasn't always possible for the R matrix. The importance of such factor for performance was left as an optimization result. If Eq. (14) couldn't be solved, the value that minimized it was used instead. The R matrix is also always invertible so as to allow Eq. (14) to be computed. This was done by making it symmetric, also reducing the number of R variables from 16 to 10.

The Q matrix was taken as being entirely null bar the main diagonal. This choice was made to decrease the number of optimization variables.

4.3 Optimization of SDRE Variant

In the SDRE variant, the R matrix had 2 terms for each R_{ij}: one constant and one proportional to the inverse of the derivative of the damping function F($\dot{v}$) in Eq. (3) with respect to $\dot{v}$. This was done so as to give more variables to the control scheme, and was motivated by the performance gain demonstrated in Saleem (2022). This makes the R matrix a function of x, as in equation (18). The factor $1/|f(x)|$ represents the local sensitivity of the damping. Greater values mean that there's a greater tendency to decrease the relative velocity, and thus less active control might be needed. Whether this is indeed a relevant metric was left for the optimization algorithm to evaluate.

$$\mathbf{R}(x) = \mathbf{R}_0 + \frac{1}{|f(x)|}\mathbf{R}_1 \tag{18}$$

This doubles the number of optimization variables from 10 to 20. As such, the SDRE system has a total of 24 variables to optimize when including the Q matrix, which is optimized in the same way as it is in the LQR system.

5. Results

The data for the vehicle model is in table (3). These values were chosen to approximate to the values in Wang *et al.* (2004), bar some rounding.

Table 3. Data for vehicle model.

Constant	Value	Constant	Value
M_s (kg)	300	M_c (kg)	30
K_s (N/m)	20 000	K_c (N/m)	200 000

To test the optimization scheme, a multi-variable optimization was performed targeting the H_2 and H_∞ metrics of the upper body. This optimization was performed with 50 individuals over 40 generations with the same parameters as the main one. The code used was able to optimize the validation case, with convergence being obtained after only 30 generations.

5.1 Convergence

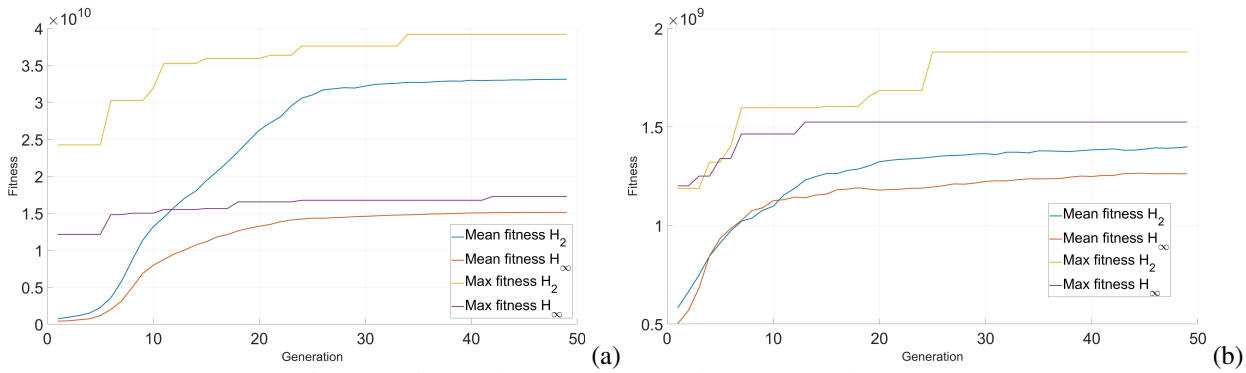

Figure 2. Fitness change over generations (a) LQR (b) SDRE.

The fitness value is a value proportional to 1 over the analyzed metric, with the absolute values being scaled for visualization purposes.

5.2 Results of the LQR optimization

The results for the NSGA-II optimization for the LQR case as well as the Pareto front are presented in Fig. (3).

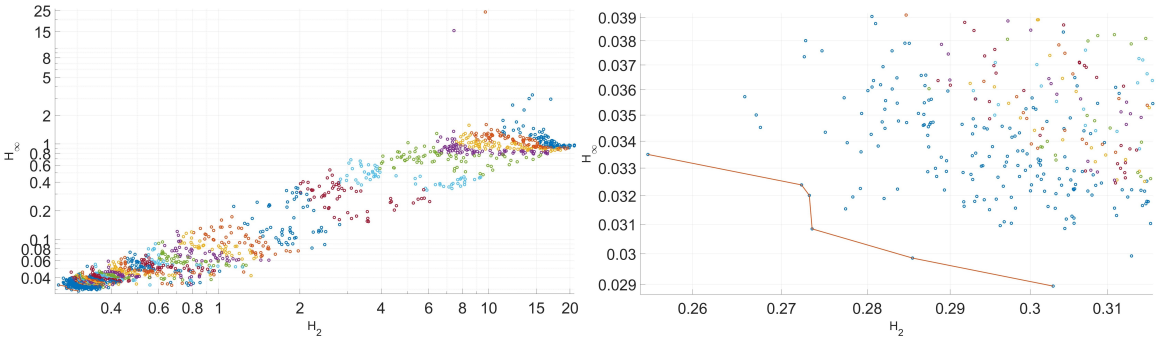

((a)) ((b))

Figure 3. Results for the NSGA-II optimization of the LQR model (a) Global (b) Zoom to the Pareto front.

Table (4) present an example of an individual picked from the Pareto optimum region.

Table 4. Example of an optimum individual for the LQR model. Individual from the Pareto front.

$R0$	1462	3842	2350	4483	Q	3072
	3842	3681	1056	1895		4082
	2350	1056	1164	1284		3504
	4483	1895	1284	728		3537

5.3 Results of the SDRE optimization

The results for the NSGA-II optimization for the SDRE case as well as the Pareto front are presented in Fig. (4).

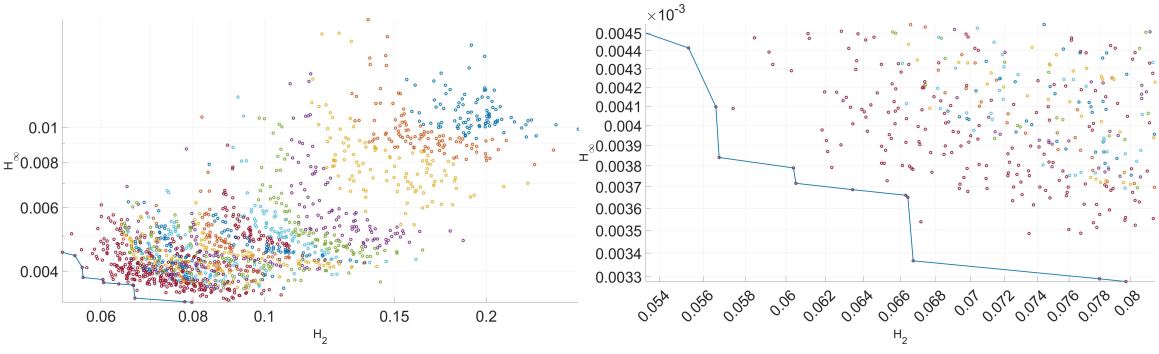

((a)) ((b))

Figure 4. Results for the NSGA-II optimization of the SDRE model (a) Global (b) Zoom to the Pareto front.

Table (5) present an example of an individual picked from the Pareto optimum region.

Table 5. Example of an optimum individual for the SDRE model. Individual from the Pareto front.

R_0	2805	1206	4300	1720	R_1	1565	2290	4169	1628	Q	3758
	1206	3669	1381	3153		2290	336	1593	2675		734
	4300	1381	2337	1794		4169	1593	2757	2640		1484
	1720	3153	1794	479		1628	2675	2640	1795		3532

5.4 Discussion of the results

The optimization resulted in a filled matrix which made use of both the R_0 and R_1. Both results were robust with respect to changes in the matrix coefficients, and small alterations didn't cause noticeable changes in performance. The resulting matrices for R_0 and R_1 are not always invertible, nor was it always possible to solve Eq. (14). The results reached the Pareto optimum after around 25 iterations, with further generations only filling up the frontier. The frontier was non-convex in both cases.

The linear damper chosen for comparison has a damping coefficient c_s of 90 500$N/(m/s)$, the average damping coefficient of the passive MR damper obtained from measurements. Comparing the points at the SDRE's and LQR's Pareto Frontiers which displayed the best H_2 with the uncontrolled MR damper and linear damper performance, it's visible that there's an improvement in both the steady-state displacement and the overall displacement due to disturbances for both cases. The constraint of maximum displacement also guaranteed that the system reached steady state much quicker, demonstrating that the controlled systems do reach steady state in 6 seconds as the optimization assumed. These results are showcased in Fig. (5).

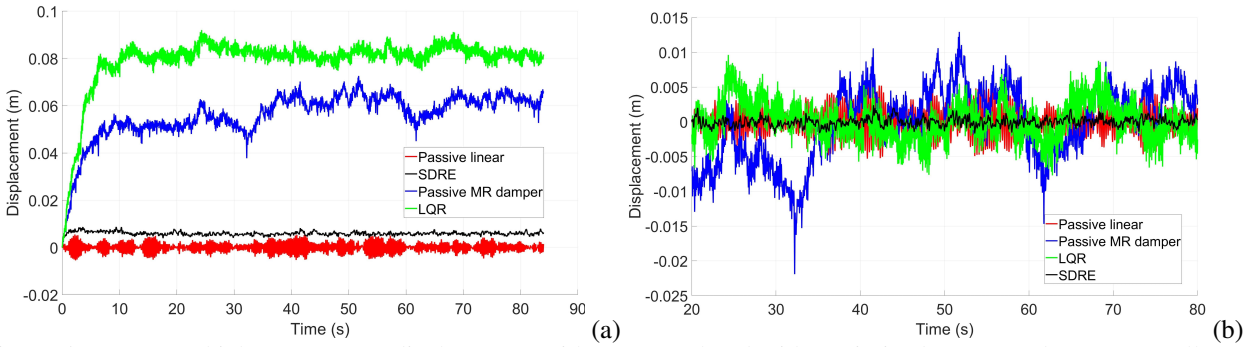

Figure 5. Quarter vehicle upper mass displacement with no control and with Optimized SDRE and LQR controllers (a) Time domain results (b) Time domain results, steady state, subtracted from their respective means.

The systems with a MR damper had non-zero displacement due to the asymmetric force properties of the damper. The SDRE controller was able to minimize such displacement, while the LQR system was unable to. All metrics were calculated relative to the steady-state equilibrium displacement.

The RMS decreased to 11% of the passive case RMS when employing the SDRE controller. This is better than the results obtained in Ferreira *et al.* (2022), Nagarkar and Vikhe (2016), and Kilicaslan (2022). Given the latter 2 are active systems, this is significant. The LQR controller, however, failed to perform better than the passive system in the RMS metric, attaining a performance 2x worse. These results are synthesized in table 6.

Table 6. Performance comparison between the present and selected works, best H_2 individuals. Ratios are between the passive and optmized cases of each respective work.

Paper	RMS ratio	H_∞ ratio	Suspension type
Ferreira *et al.* (2022) (Groundhook)	520%	87%	Semi-active
Ferreira *et al.* (2022) (Skyhook)	87%	97%	Semi-active
Nagarkar and Vikhe (2016)	66%	-	Active
Kilicaslan (2022)	50%	-	Active
SDRE (present)	11,4%	7,8%	Semi-active
LQR (present)	213%	50%	Semi-active
MR damper (present)	770%	50%	Semi-active

Unlike with the hook family of control schemes, there was a simultaneous improvement of the RMS and Roadhold, with values 2 orders of magnitude smaller for the latter. The LQR controller was not able to achieve significant RMS improvements, but it was able to outperform the Groundhook scheme. As such, the tested control schemes are better at handling both safety and comfort simultaneously.

The value of 11% should be taken within context. While it outperformed the active systems in the improvement over the passive case, the passive damper coefficient was far above the ideal coefficient that's suggested in the literature (Gillespie, 1992). The ideal value for this system is 4899 $N/(m/s)$, making the tested passive system overdamped. As such, the

lesser improvements experienced in other works might be partially due to a better passive system leaving less room for performance improvements.

6. Conclusion and perspectives

The present work compared the behavior of a semi-active suspension using the LQR and SDRE schemes. Both of the employed techniques were successful in reducing the metrics of interest, improving the vehicle safety and comfort characteristics. The SDRE technique provided greater improvements to the performance of the system, justifying it's implementation over the traditional LQR approach, as well as over a passive solution.

The proposed modification for the SDRE cost matrix was successful at further improving performance. The solution to the problem was shown to be non-trivial, as the resulting control matrices were full. However, optimization of the suspension controller can be further bolstered by optimizing the suspension properties themselves. As such, the optimization of the suspension physical parameters was identified as very important to obtain performance improvements beyond a limit.

The obtained controllers can be applied on real-time systems. However, there was no analysis on the robustness of the controller with respect to changes in the damper properties, being a possible short-coming in real world applications.

Future studies may evaluate the simultaneous optimization of both the controller characteristics and the suspension properties, making it possible for a true optimal solution to be found. The control of more complex vehicle models, such as the half-vehicle or the full vehicle model, can also be explored, as whether the SDRE controller can balance their greater number of metrics well is not yet known. The performance of the SDRE controller can also be compared to other modern approaches to non-linear control, with Lyapunov based methods such as back stepping and sliding modes being good candidates for further analyses, as they have been employed in the design of active suspensions with great success.

7. REFERENCES

Acarman, T., 2009. "Nonlinear optimal integrated vehicle control using individual braking torque and steering angle with on-line control allocation by using state-dependent riccati equation technique". *Vehicle System Dynamics*, Vol. 47, No. 2, pp. 155–177. doi:10.1080/00423110801932670.

Aguilar-Ibanez, C., Jimenez-Lizarraga, M.A., Gandarilla-Esparza, I., Moreno-Valenzuela, J., Saldivar, B., Suarez-Castanon, M.S. and Rubio, J.d.J., 2022. "Robust velocity and load observer for a general noisy rotating machine". *Machines*, Vol. 10, No. 11. ISSN 2075-1702. doi:10.3390/machines10111009. URL https://www.mdpi.com/2075-1702/10/11/1009.

Chen, M.Z., Hu, Y., Li, C. and Chen, G., 2014. "Semi-active suspension with semi-active inerter and semi-active damper". *IFAC Proceedings Volumes*, Vol. 47, No. 3, pp. 11225–11230. ISSN 1474-6670. doi:https://doi.org/10.3182/20140824-6-ZA-1003.00138. URL https://www.sciencedirect.com/science/ARTICLE/pii/S1474667016434002. 19th IFAC World Congress.

Cloutier, J.R., D'Souza, C.N. and Mracek, C.P., 1996. "Nonlinear regulation and nonlinear h control via the state-dependent riccati equation technique: Part 1, theory". In *Proceedings of the international conference on nonlinear problems in aviation and aerospace*. Embry Riddle University Press, Daytona Beach, Florida, pp. 117–131.

Cloutier, J., 1997. "State-dependent riccati equation techniques: an overview". Proceedings of the 1997 American Control Conference (Cat. No.97CH36041), Vol. 2, pp. 932–936. doi:10.1109/ACC.1997.609663.

de Lima, J.G.M., de Morais, M.V.G. and de Araújo, M.L., 2012. "Avaliação qualitativa do comportamento não linear de modelo de meio veículo". *VII Congresso Nacional de Engenharia Mecânica*.

Deb, K., Agrawal, S., Pratap, A. and Meyarivan, T., 2000. "A fast elitist non-dominated sorting genetic algorithm for multi-objective optimization: Nsga-ii". In M. Schoenauer, K. Deb, G. Rudolph, X. Yao, E. Lutton, J.J. Merelo and H.P. Schwefel, eds., *Parallel Problem Solving from Nature PPSN VI*. Springer Berlin Heidelberg, Berlin, Heidelberg, pp. 849–858.

Do, T.D., Choi, H.H. and Jung, J.W., 2012. "Sdre-based near optimal control system design for pm synchronous motor". *IEEE Transactions on Industrial Electronics*, Vol. 59, No. 11, pp. 4063–4074. doi:10.1109/TIE.2011.2174540.

Ferreira, L.C.R., de Morais, M.V.G. and Avila, S.M., 2022. "Parametric optimization of quarter vehicle suspension model by response map technique". In *Proceedings of the XLIII Ibero-Latin-American Congress on Computational Methods in Engineering*. ISSN 2675-6269. URL https://cilamce.com.br/anais/arearestrita/2022/11262.pdf.

Ferreira, L.C.R., de Morais, M.V.G. and Avila, S.M., 2023. "Modelling mr dampers under non-harmonic excitations through logistic curve models [manuscript in preparation]". In *Proceedings of the XLIV Ibero-Latin-American Congress on Computational Methods in Engineering*.

Ferreira, L.C.R., 2022. "Modelagem dinâmica do comportamento de amortecedores magnetoreologico para aplicação em suspensão veicular semi-ativa". Trabalho de Conclusão de Curso (Bacharelado em Engenharia Mecânica) —

Universidade de Brasília. URL https://bdm.unb.br/handle/10483/34746.

Gawronski, W., 2004. *Advanced Structural Dynamics and Active Control of Structures*. Springer, 1st edition.

Gillespie, T.D., 1992. *Fundamentals of Vehicle Dynamics*.

Gomes, P.C. and de Morais, M.V.G., 2021. "Parametric optimization of tmd inerter for vibration control of vehicle suspension".

Itik, M., Salamci, M.U. and Banks, S.P., 2010. "Sdre optimal control of drug administration in cancer treatment". *Turkish Journal of Electrical Engineering and Computer Sciences*, Vol. 18, No. 5, pp. 715–730.

Kilicaslan, S., 2022. "Control of active suspension system in the presence of nonlinear spring and damper". *Scientia Iranica*, Vol. 29, No. 3, pp. 1221–1235. ISSN 1026-3098. doi:10.24200/sci.2021.58189.5607. URL https://scientiairanica.sharif.edu/ARTICLE_22475_cc1d34a4ba6032fdbd864385f8e6f37f.pdf.

Koch, G.P.A., 2011. *Adaptive Control of Mechatronic Vehicle Suspension Systems*. Master's thesis, TECHNISCHE UNIVERSITÄT MÜNCHEN.

Li, W., Dong, X., Yu, J., Xi, J. and Pan, C., 2021. "Vibration control of vehicle suspension with magneto-rheological variable damping and inertia". *Journal of Intelligent Material Systems and Structures*, Vol. 32, No. 13, pp. 1484–1503. doi:10.1177/1045389X20983885. URL https://doi.org/10.1177/1045389X20983885.

Md Sam, Y., Ab Ghani, M.R. and Ahmad, N., 2000. "Lqr controller for active car suspension". Vol. 1, pp. 441 – 444 vol.1. ISBN 0-7803-6355-8. doi:10.1109/TENCON.2000.893707.

Melo, M.A., 2017. *Análise Comparativa de Estratégias para Suspensão Semiativa em um Modelo de 1/4 de Veículo*. Master's thesis, Universidade de Brasilia.

Morar, D. and Dobra, P., 2021. "Optimal lqr weight matrices selection for a cnc machine controller". In *2021 23rd International Conference on Control Systems and Computer Science (CSCS)*. pp. 21–26. doi:10.1109/CSCS52396.2021.00011.

Nagarkar, M.P. and Vikhe, G.J., 2016. "Optimization of the linear quadratic regulator (LQR) control quarter car suspension system using genetic algorithm". *Ingeniería e Investigación*, Vol. 36, pp. 23 – 30. ISSN 0120-5609. URL http://www.scielo.org.co/scielo.php?script=sci_arttext&pid=S0120-56092016000100004&nrm=iso.

Ogata, K., 2011. *Modern Control Engineering*. Pearson Prentice Hall. ISBN 9788576058106.

Prabakar, R.S., Sujatha, C. and Narayanan, S., 2016. "Response of a half-car model with optimal magnetorheological damper parameters". *Journal of Vibration and Control*, Vol. 22, No. 3, pp. 784–798. doi:10.1177/1077546314532300. URL https://doi.org/10.1177/1077546314532300.

Proakis, J.G. and Manolakis, D.G., 1996. *Digital Signal Processing (3rd Ed.): Principles, Algorithms, and Applications*. Prentice-Hall, Inc., USA. ISBN 0133737624.

Saleem, O., 2022. "An enhanced adaptive-lqr procedure for under-actuated systems using relative-rate feedback to dynamically reconfigure the state-weighting-factors". *Journal of Vibration and Control*. doi:10.1177/10775463221078654. URL https://doi.org/10.1177/10775463221078654.

Santade, F., 2017. *Análise dinâmica de amortecedores não lineares assimétricos, com histerese e sujeitos a folga e avaliação do efeito temperatura*. Master's thesis, Universidade Estadual Paulista.

Shirahatti, A., Prasad, P., Panzade, P. and Kulkarni, M., 2009. "Optimal design of passenger car suspension for ride and road holding". *Journal of the Brazilian Society of Mechanical Sciences and Engineering [online]*, Vol. 30, pp. 66–76. doi:https://doi.org/10.1590/S1678-58782008000100010.

Silva, D.M., Morais, M. and Avila, S., 2022. "Sistema de suspensão semi-ativa automotiva utilizando amortecedor magneto-reológico". doi:10.5944/bicim2022.067.

Stansbery, D. and Cloutier, J., 2001. *Nonlinear, hybrid bank-to-turn/skid-to-turn missile autopilot design*. AIAA Guidance, Navigation, and Control Conference and Exhibit. doi:10.2514/6.2001-4158. URL https://arc.aiaa.org/doi/abs/10.2514/6.2001-4158.

Wang, E.R., Ma, X.Q., Rakheja, S. and Su, C.Y., 2004. "Modeling asymmetric hysteretic properties of an mr fluids damper". *43rd IEEE Conference on Decision and Control*.

Wei, C. and Taghavifar, H., 2017. "A novel approach to energy harvesting from vehicle suspension system: Half-vehicle model". *Energy*, Vol. 134, pp. 279–288. ISSN 0360-5442. doi:https://doi.org/10.1016/j.energy.2017.06.034. URL https://www.sciencedirect.com/science/ARTICLE/pii/S0360544217310289.

Zhang, X., Ahmadian, M. and Guo, K.H., 2012. "On the benefits of semi-active suspensions with inerters". *Shock and Vibration*, Vol. 19, pp. 257–272. doi:10.1155/2012/640275.

Çimen, T., 2010. "Systematic and effective design of nonlinear feedback controllers via the state-dependent riccati equation (sdre) method". *Annual Reviews in Control*, Vol. 34, No. 1, pp. 32–51. ISSN 1367-5788. doi:https://doi.org/10.1016/j.arcontrol.2010.03.001.

8. RESPONSIBILITY NOTICE

The authors are solely responsible for the printed material included in this paper.